Improving the Performance of the Space Observation Radar TIRA through Dedicated Signal Processing Techniques and Advanced Experimental Modes

Delphine Cerutti-Maori, Claudio Carloni, Jens Rosebrock, Itawel Maouloud
Fraunhofer Institute for High Frequency Physics and Radar Techniques (FHR)
GERMANY

delphine.cerutti-maori@fhr.fraunhofer.de

ABSTRACT

The Tracking and Imaging Radar (TIRA) is a powerful space observation radar, which combines a tracking radar and an imaging radar. A dynamic 34 m parabolic antenna confers its high sensitivity and agility to detect, track and image space objects on the system. Originally developed in the 70s and 80s, the system has been continuously upgraded over the years to meet the increasing requirements on sensors for Space Situational Awareness (SSA). This paper presents some recent achievements dealing with the goal of improving the performance of the TIRA system through tailored signal processing techniques without modifying the system hardware.

1.0 INTRODUCTION

The Tracking and Imaging Radar (TIRA) system [1-3], which is developed and operated at Fraunhofer FHR, is a powerful space observation radar. It combines a tracking radar in L-band and an imaging radar in Ku-band with a high-gain reflector antenna of 34 m diameter. It is used for a variety of tasks in the field of Space Situational Awareness (SSA) ranging from the detection of small pieces of debris, the tracking of space objects for precise orbital measurement, up to the imaging of these objects. Since its first development phase in the 70s, the TIRA system has been widely commissioned by the German SSA Center (GSSAC) and diverse space agencies for reconnaissance, mission support, and space debris characterization. In order to improve the quality of the delivered data, the system has been continuously upgraded over the years.

The tracking radar operates with a center frequency of 1.33 GHz. It is equipped with a monopulse system allowing a real-time estimation of the azimuth and elevation angles of an object located in the main beam of the antenna. The system uses currently Doppler intolerant waveforms coded according to the Binary Phase Shift Keyed (BPSK) principle [4]. The number of subpulses, which determines the range resolution, is set by the system in real-time during the tracking according to the measured Signal-to-Noise Ratio (SNR). At present, the system requires an a-priori knowledge of the object parameters (Two-Line Element (TLE) set) in order to track the object. Knowing the expected range and Doppler frequency of the object, the true parameters are computed using a correlator quartet similar to the monopulse principle. The PRF of the tracking radar is usually around 30 Hz and is adjusted automatically by the system to ensure that the receive signal falls in the receive window. During the observation of a space object, the radar transmits a pulse sequence. For each single pulse, which is associated to a given epoch, an observation vector is generated (single pulse detection). This raw observation vector includes the measured range, range rate, azimuth and elevations angles, as well as the SNR from which the Radar Cross Section (RCS) of the object can be derived [5]. A smoothing is applied to the raw observation vectors to generate the final observation vectors that are delivered to our partners. An example of a typical measurement protocol is shown in Figure 1-1. Accurate orbital parameters of a space object can be gained from a series of observation vectors finding applications e.g. for orbit determination, re-entry forecast, and collision risk analysis.

The tracking radar controls the imaging radar, which operates at a center frequency of 16.7GHz. The imaging radar uses linear frequency modulated (chirp) waveforms [4]. For each transmitted radar pulse, a

range profile of the object is measured. Using the Inverse Synthetic Aperture Radar (ISAR) principle [6], a radar image can be computed by spectral analysis of a sequence of consecutive range profiles. The ISAR principle exploits the variation of the range of the different point scatterers of the object over time to generate 2D radar images. Figure 1-2 shows an example of an ISAR image from the same observation as Figure 1-1. From a series of radar images, it is possible to assess the attitude motion of the object under the assumption of a fixed rotational velocity vector over the observed passage or part of it. A 3D Wire Grid Model (WGM) is first generated for the observed object. The WGM is then manually fitted to some selected ISAR images. An optimization procedure based on a Maximum Likelihood (ML) approach [7] searches for the initial attitude and rotational velocity vector that best match the manually projected WGM [8,9]. Information about e.g. shape and size of objects, their status (damaged or undamaged), intrinsic motion (stabilized or tumbling), characteristics (technical analysis) can be derived from a series of radar images.

Lately, efforts were undertaken in order to improve the actual performance of the space observation radar TIRA through the development of tailored signal processing techniques and advanced observation modes without modifying the system hardware. This paper describes some recent achievements. Section 2 presents an experimental high-resolution observation mode yielding observation vectors of improved quality. Section 3 is dedicated to the discrimination of several objects located simultaneously in the radar beam. Finally, Section 4 discusses some fields of applications for SSA and improvements for operation support.

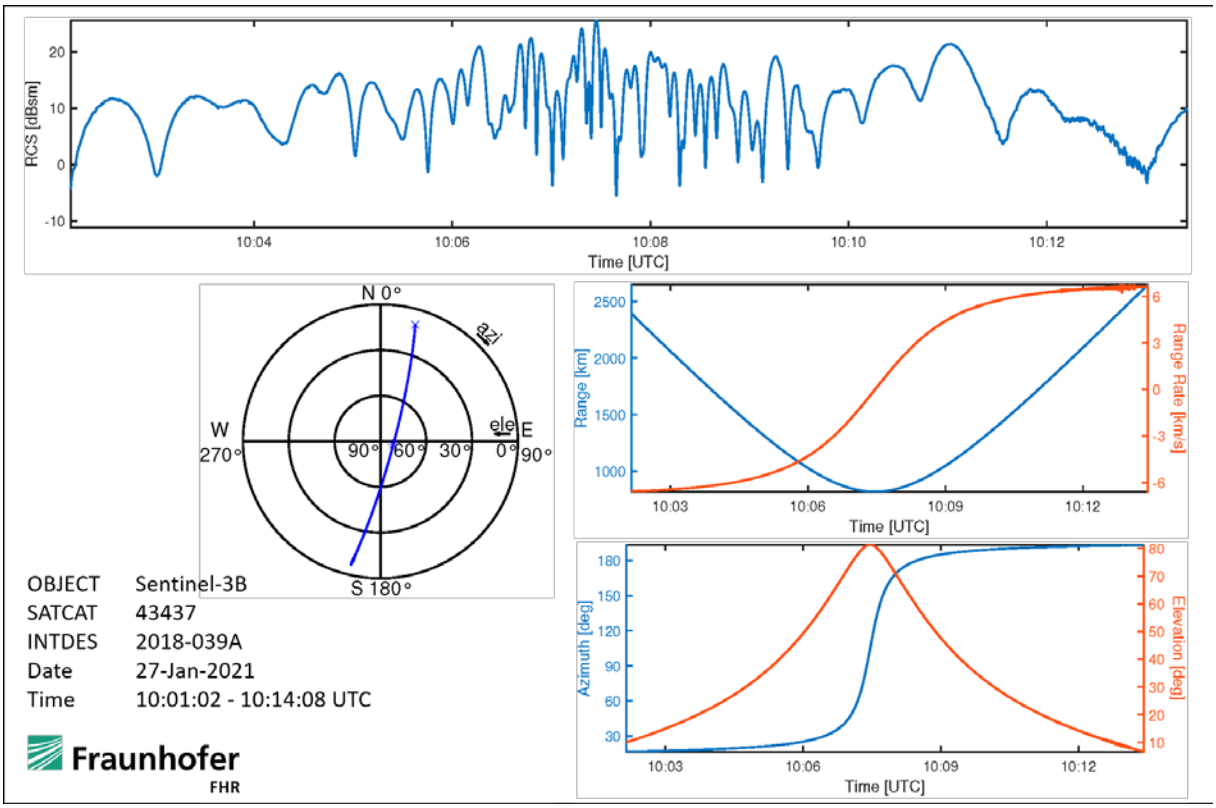

Fig. 1-1 – An exemplary measurement protocol.

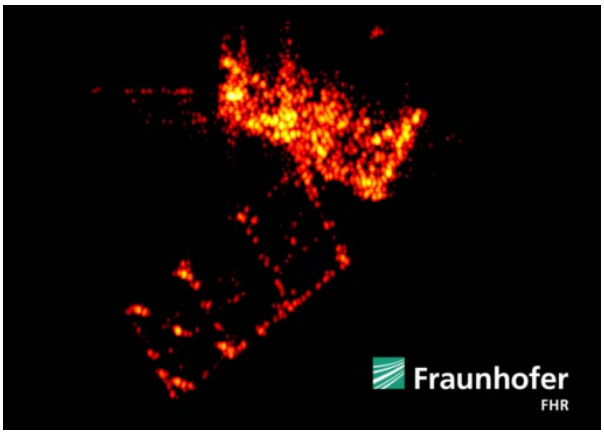

(a) ISAR image of Sentinel-3B (from [10]).

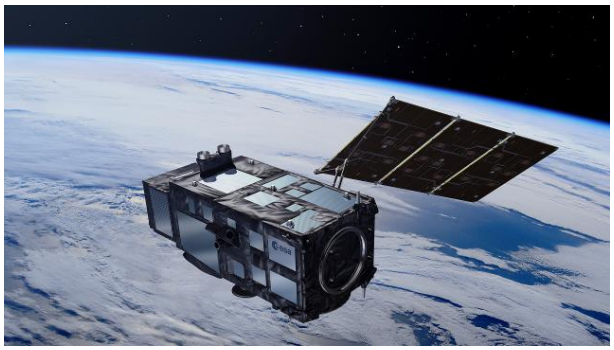

(b) Sentinel-3 satellite (© ESA).

Fig. 1-2 – Typical radar image (from the same observation as Figure 1-1).

2.0 EXPERIMENTAL HIGH-RESOLUTION OBSERVATION MODE

2.1 Objective

A major task of SSA is to know about the objects in orbit and to predict their position at a given time in the future. SSA relies on the acquisition of orbital data by a variety of sensors such as optical sensors, laser systems, and radar systems in a monostatic or in a bi/multistatic configuration [11]. The better the measurement quality of these systems, the better the derived orbital data.

During recent research activities, the possibility of increasing the accuracy of the delivered observation vectors and of estimating additional parameters that could be beneficial for SSA was examined. The investigations resulted in the proof of concept of a high-resolution observation mode, which is currently under development [12]. This experimental mode finds use, when highly accurate observation data are necessary, e.g. for collision avoidance. It uses the data measured by the two radars combined with a novel processing scheme based on coherent integration and data fusion. Calibration measurements have shown that the estimation accuracy of the range could be improved by a factor 35 and the estimation accuracy of the range rate by a factor 5 [12]. Another parameter, the range rate rate, can be also derived, which can be exploited for Initial Orbit Determination (IOD) [13].

2.1.1 Range

Since the bandwidth of the imaging radar is larger than the one of the tracking radar, a more accurate measurement of the range can be gained with the imaging radar. However, since the waveform used by the imaging radar (chirp) is Doppler tolerant and shows an ambiguity between range and Doppler frequency, the measured data have to be corrected first. After compensation of the undesirable phase terms, a second measurement of the object range can be derived (Figure 2-1 (a)). Both measurements can be fused together yielding a refined range measurement.

2.1.2 Range rate and range rate rate

As explained before, the range rate, which is proportional to the Doppler frequency, is determined by the correlation quartet. The main beam of the ambiguity function centered on the expected range and Doppler frequency of the object is sampled at four different positions, from which the range rate is computed. Since

the predicted object parameters differ from the true parameters, the estimated range rate is slightly biased.

A new processing scheme was developed to improve the range rate measurement and, at the same time, estimate the range rate rate. It is based on a three-step processing of the raw tracking radar data. In a first step, a weighted Least Square (LS) is used to obtain a rough estimate of the range rate and range rate rate over several pulses. Then, in a second step, a multivariate beamformer is applied to the data to search for the range rate and range rate rate that best fit the data according to an ML approach (Figure 2-2). Since the PRF is low and the object RCS is sometimes not sufficiently high, the rough range rate estimate may differ from the true range rate by more than the ambiguous range rate value. The third step seeks to solve this issue. Figure 2-1 (b) and (c) show the obtained range rate and range rate rate residuals for a calibration measurement.

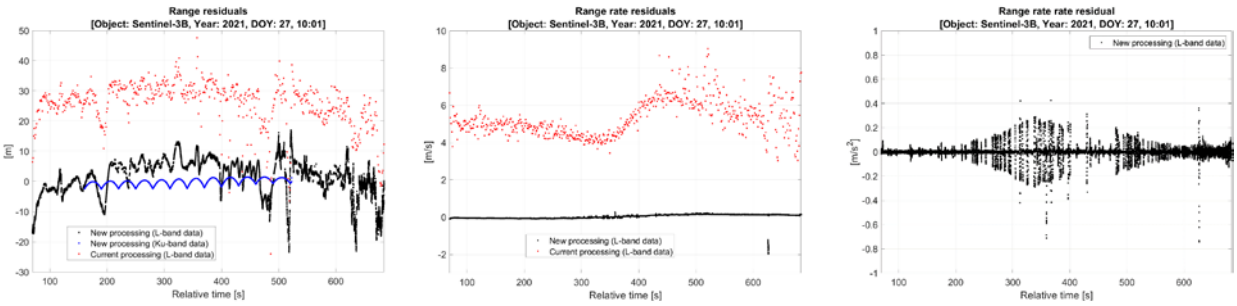

(a) Range residuals for a calibration measurement of Sentinel-3B

(b) Range rate residuals for a calibration measurement of Sentinel-3B

(c) Range rate rate residual for a calibration measurement of Sentinel-3B

Fig. 2-1 – Different observables (from [12]). The current processing is indicated in red and the new processing in black (tracking radar data) and in blue (imaging radar data).

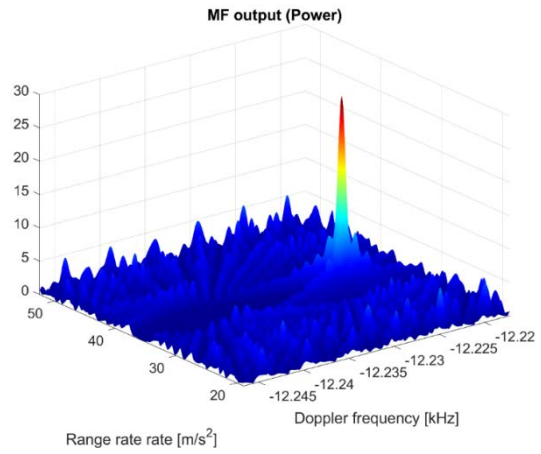

Fig. 2-2 – Matched filter output (data of Figure 2-1).

2.2 IOD

So far, we assumed that the orbital data of the object were known. Without this knowledge, the TIRA system cannot track a space object. A future goal is to track an object without any a priori knowledge about the

object TLE. This could be interesting after a fragmentation to track large pieces of debris. Another application could be the tracking of hostile satellites after their detection. Such an autonomous tracking mode [14] requires an initialisation phase during which first orbital data are gained. This IOD phase is particularly challenging for the TIRA system due to the narrow antenna beam.

An IOD method was developed that exploits the range rate rate parameter, which was previously introduced. This observable gives information about the velocity of the object. Combined with the radial velocity and the angular information, the velocity vector can be fully determined. Figure 2-3 shows a comparison of the performance of this IOD method with the Herrick-Gibbs method [15,16]. A linear fit according to [17] was performed on the raw observation vectors before being processed by the Herrick-Gibbs method. This is done in order to consider all the observations vectors and not only 3 of them. One can observe that the best overall performance is achieved for the method exploiting the range rate rate parameter [13]. An improvement is noticed for both observation arcs.

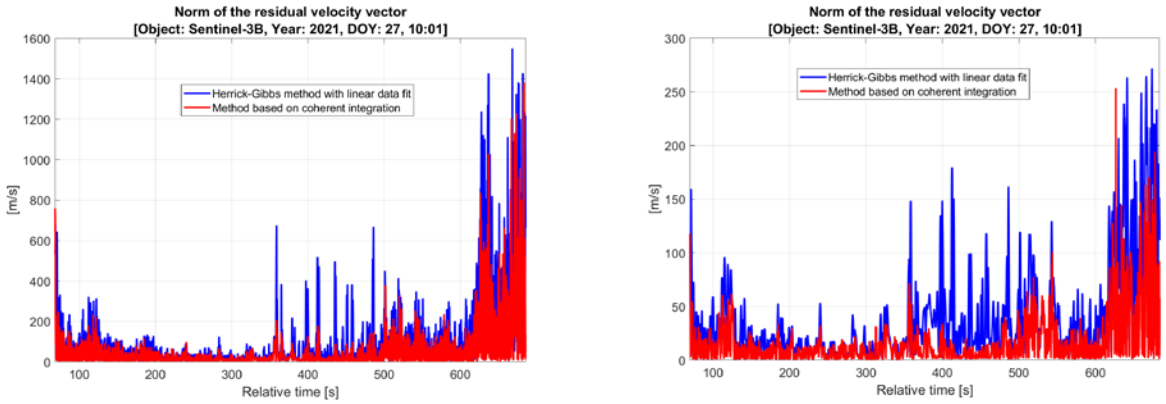

(a) Processing interval 2 s.

(b) Processing interval 5 s.

Fig. 2-3 – Comparison of different IOD techniques (data of Figure 2-1).

3.0 SEPARATION OF MULTIPLE OBJECTS

3.1 Objective

A challenging task for SSA is to detect and identify hostile objects in the surrounding of an allied satellite. The hostile object could pose a serious threat by spying the allied satellite or by purposely destroying it. Critical situations happened previously such as the approach of the Franco-Italian military satellite Athena-Findus by a Russian satellite in 2017. Another critical SSA task is the surveillance of the early phase of space missions. It is common that several objects are launched simultaneously. However, the “official” number of launched objects may differ from the true number. One could speculate the launch of a hostile satellite. Such situations could be monitored by radar systems.

When the distance between the objects is large enough but both objects are in the antenna beam of a tracking radar, the objects are located into different range/Doppler cells and can be consequently discriminated (Figure 3-1 (a)). When the objects are close enough to each other, an imaging radar can image both objects simultaneously, allowing their discrimination (Figure 3-1 (b)). However, a critical phase is when the aforementioned conditions are not fulfilled (Figure 3-1 (c)). In this case, the objects have similar orbital data and the different echoes acquired by the tracking radar fall in the same range/Doppler cell after matched filtering. In addition, their distances are such that they cannot be imaged simultaneously. Their cross-range distances are larger than the beam-footprint of the imaging radar and/or the backscattered signals are not

contained in the range receive window.

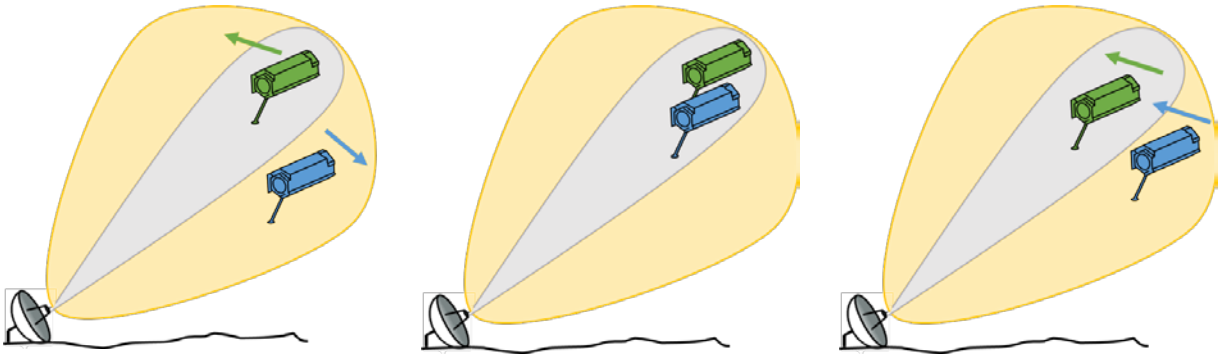

(a) Case 1: The signals backscattered by the two objects are located into different range/Doppler cells (tracking radar).

(b) Case 2: Both objects can be imaged simultaneously (imaging radar).

(c) Case 3: The signals backscattered by the two objects fall in the same range/Doppler cell (tracking radar).

Fig. 3-1 – Different cases for discriminating multiple objects. The antenna beamwidth of the imaging radar (grey) is smaller compared to the one of the tracking radar (yellow) due to the higher operating frequency.

In order to discriminate several objects during this critical intermediate phase, a method called monopulse dechirping was developed, which is applied in the following to Low Earth Orbit (LEO) and geostationary (GEO) objects. This method allows to separate objects in 4D plane range rate / range rate rate / azimuth angle / elevation angle.

3.2 LEO

Due to the large antenna size and the resulting high gain, the TIRA system is very sensitive and can detect and track small pieces of LEO debris, when a TLE set is available. LEO objects are moving very fast with respect to an observer on the Earth, making a coherent processing over several pulses challenging. This is caused by the low PRF with respect to the true Doppler frequency of the object and the fast variation of the range rate and range rate rate over time. This parameter variation produces decorrelation effects and limits the Coherent Processing Interval (CPI).

The Astroscale mission [18] is selected in the following as an example of multiple objects observation in the LEO regime. At the beginning of April 2022, an encounter maneuver was conducted between ELSA-D and ELSA-D CLIENT. On April 8, the distance between the two objects was expected to be around several hundreds of meters. FHR was commissioned by DLR/GSSAC to observe the two satellites with the TIRA system. However, it turned out that it was not possible to image both objects simultaneously as the cross range distance was larger than the beam footprint. Figure 3-2 shows the measured RCS (Case 3 of Figure 3-1). The oscillation with changing frequency and amplitude clearly indicates that several objects are located simultaneously in the radar beam. The waves backscattered by each object are coherently added explaining the observed modulated signal. A big challenge for discriminating the two objects is their size difference. ELSA-D (about 100 cm × 70 cm × 70 cm) is much larger compared to ELSA-D CLIENT (about 50 cm × 50 cm × 20 cm). The SNR of the receive signals is expected to differ by more than 10-15 dB, complicating the target detection due to sidelobe effects. Figure 3-3 presents the results after matched filter at three different instants of time. The larger response corresponds to the signal of ELSA-D. Since the RCS of an object can strongly vary over time (e.g. according to the incidence angle), it is possible in some cases to detect ELSA-D

CLIENT (Figure 3-3 (a) and (b)). Note that the estimated relative range rate can be ambiguous by a multiple of 3.4 m/s due to the low PRF.

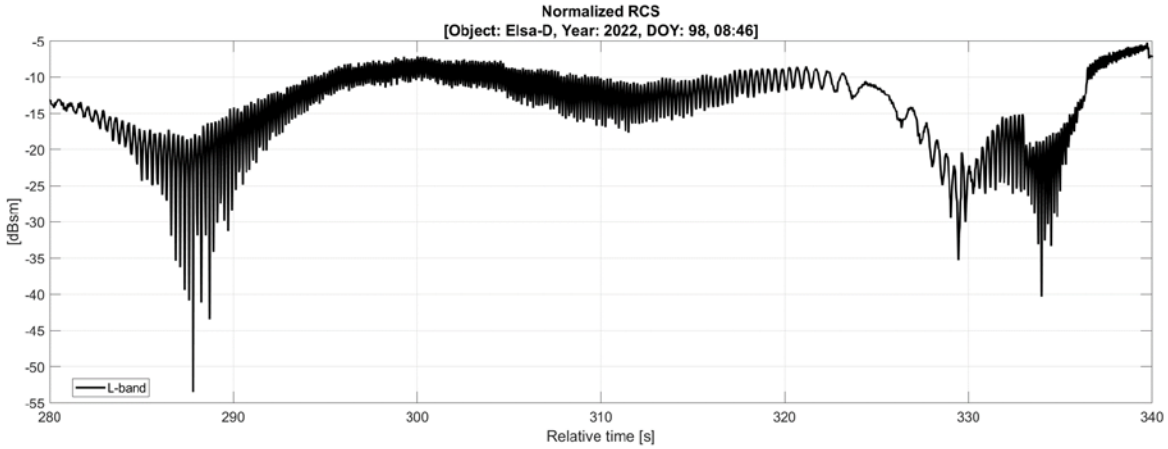

Fig. 3-2 – Measured RCS.

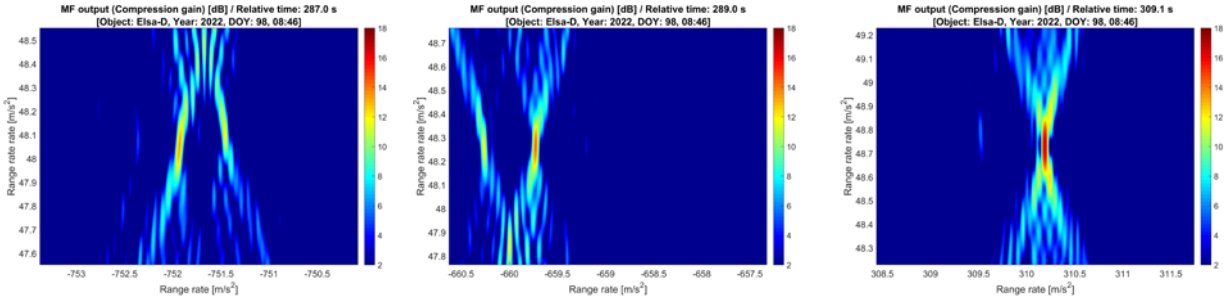

(a) Relative time: 287.0s (b) Relative time: 289.0s (c) Relative time: 309.1s

Fig. 3-3 – Matched filter output after integration over 2 s.

3.3 GEO

The detection of GEO objects with radar systems is quite challenging due to the low SNR caused by the long range around 36000 km. With the TIRA system it is generally not possible to detect a GEO object from a single pulse. Several pulses have to be coherently integrated to increase the sensitivity. GEO objects have the advantage of stationarity over LEO objects. The range rate is almost constant over several seconds and it is (usually) not necessary to correct any phase variation caused by the range rate rate.

Within the NATO Sensors, Electronics and Technology (SET) Research Task Group (RTG) (SET-293), several deep space observations were conducted between several NATO partners within Europe and in the USA with the aim of improving SSA capability by exploiting monostatic and bistatic measurements [19]. The TIRA system and the Millstone Hill Radar in the USA transmitted radar signals, which were backscattered by selected GEO satellites and received by several radio telescopes distributed all over Europe. Figures 3-4 and 3-5 show the monostatic results achieved with the TIRA system for the observation of Alcomsat-1 (43039 / 17078A) on May 7, 2021. The mean SNR of the raw data is around ~0 dB, which is too

low for single pulse detection. The results after integration over 8 s using the method described in [10] are shown in Figure 3-4. The response of Alcomsat-1 is clearly visible on the left. Another object with a weaker signal could be detected on the right. This object could not be identified yet by cross correlating the TLE catalogue downloaded at the time prior to the experiment. This object could have performed a maneuver explaining the unsuccessful correlation. Conducting a threshold detection based on a CLEAN-like method [20] and a detection clustering on the matched filter results, a detection list can be generated. The relative range rate and range rate rate of the objects can be accurately estimated (Figure 3-5 (a) and (b)). The drift observed in in Figure 3-5 (a) for object 2 supports the hypothesis of the maneuver. It is also possible to estimate the Line-Of-Sight (LOS) of the objects from the monopulse ratio (Figure 3-5 (d)). The variance is in agreement with the estimated SNR (Figure 3-5 (c)).

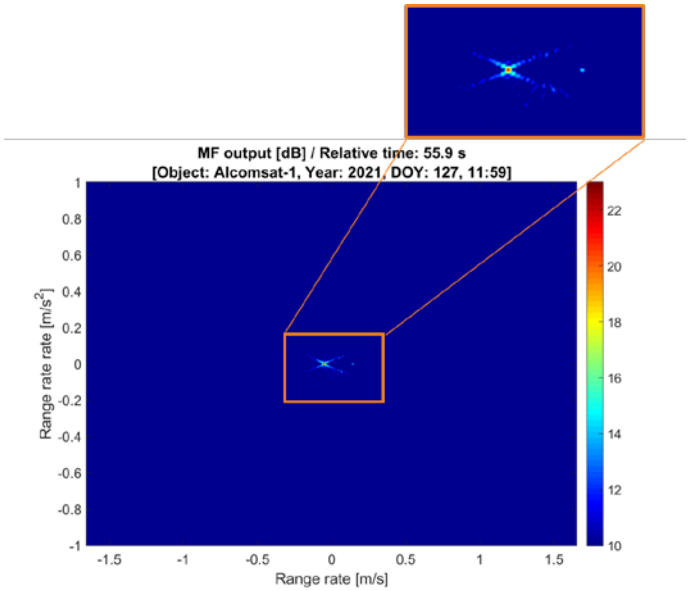

Fig. 3-4 – Matched filter output after integration over 8 s.

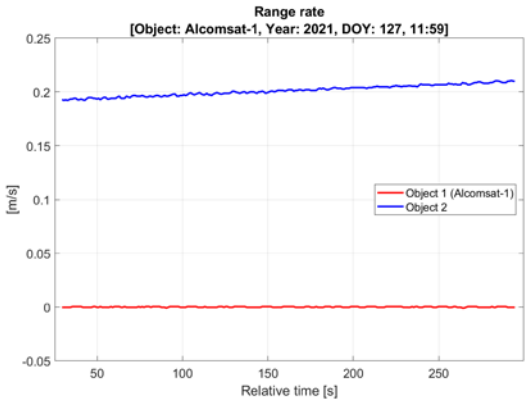

(a) Estimated range rate.

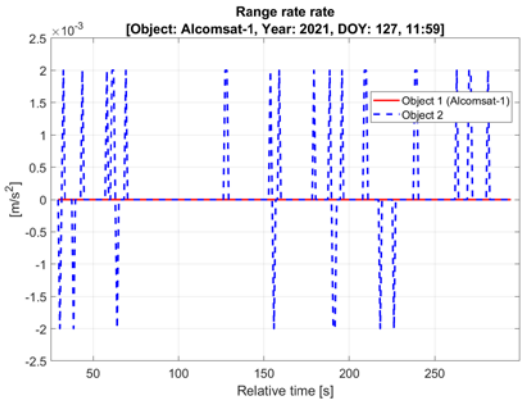

(b) Estimated range rate rate.

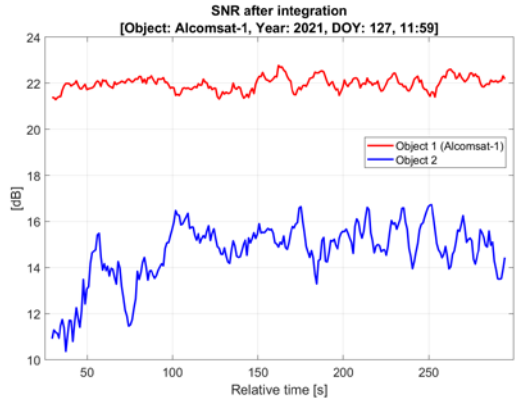

(c) Estimated SNR after integration.

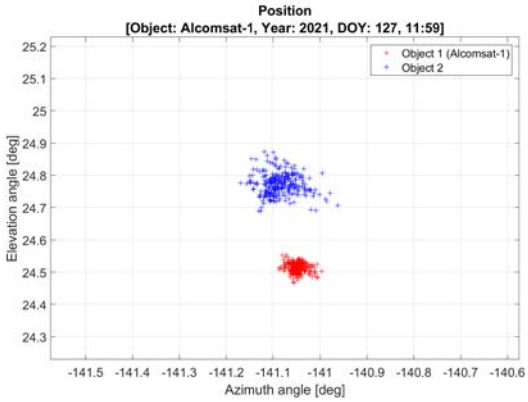

(d) Estimated azimuth and elevation angles.

Fig. 3-5 – Estimated parameters.

4.0 CONCLUSIONS

In this paper, signal processing techniques based on coherent integration were presented and discussed in order to upgrade the performance of the space observation radar TIRA without modifying the system hardware. In particular, an experimental high-resolution observation mode was introduced to obtain measurement data of improved accuracy. This mode combines the data acquired by the two radars of the TIRA system in order to refine the range measurement. A new coherent processing of the tracking radar data enables to increase the accuracy of the range rate measurement and to determine a new parameter, the range rate rate. Variations of this techniques can be tailored to the LEO and GEO regimes to discriminate several objects in the radar beam. This processing can also be applied to the different receive channels of a multi-channel radar to estimate the object LOS, as in the case of the recently developed monopulse dechirping technique.

Fields of applications for SSA of these new techniques are numerous and an improvement for operation support is expected. Measurement data of higher accuracy allows improving the quality of the derived orbital products. This can be particularly interesting e.g. for computing collision probabilities between space objects leading to the execution (or not) of costly collision avoidance manoeuvres. First orbital information of newly detected objects, which are not contained in any catalogue, could be gained by exploiting the range rate rate parameter giving information about the object velocity. Finally, discriminating several objects and

determining their relative motion and position over time is a major SSA competency, e.g. during mission start or in order to detect and track potentially hostile satellites in the surrounding of an allied satellite.

ACKNOWLEDGMENT

The authors would like to thank the German Ministry of Defense (MOD) and the DLR (Project D/301/67264737) for funding this activity. The authors are also thankful to the measurement team for conducting the radar observations.

REFERENCES

[1] D. Mehrholz, „Ein Verfolgungs- und Abbildungsradarsystem zur Beobachtung von Weltraumobjekten“, Frequenz, Bd. 50, Ausgabe 7-8:138–146, Juli-August 1996.

[2] D. Mehrholz, „Radardatengewinnung und Fehlerübertragung bei der Beobachtung von nichtkooperativen Objekten im erdnahen Weltraum“, PhD, Universität der Bundeswehr, 1988.

[3] D. Mehrholz, “Radar Observations of Geosynchronous Orbits”, 2nd European Conference on Space Debris, 1997.

[4] N. Levanon, E. Mozeson, “Radar Signals”, John Wiley & Sons, 2004.

[5] M. Richards, “Fundamentals Of Radar Signal Processing”, New York, NY: McGraw-Hill, 2005.

[6] Victor C. Chen, Marco Martorella, “Inverse Synthetic Aperture Radar Imaging: Principles, Algorithms and Applications”, IET, 2014.

[7] Steven M. Kay, “Fundamentals of Statistical Signal Processing, Vol. 1&2”, Prentice Hall Signal Processing Series, Alan Oppenheim, Series Editor.

[8] J. Rosebrock, “Absolute Attitude From Monostatic Radar Measurements of Rotating Objects”, IEEE Transactions on Geoscience and Remote Sensing, Vol.: 49, Issue: 10, October 2011.

[9] S. Sommer, J. Rosebrock, D. Cerutti-maori, L. Leushacke, “Temporal analysis of Envisat's rotational motion”, Proc. 7th European Conference on Space Debris, Darmstadt, Germany, 2017.

[10] F. Rosebrock, J. Rosebrock, D. Cerutti-Maori, and J. Ender, “ISAR imaging by integrated Compressed Sensing, range alignment and autofocus”, Proc. EUSAR 2021.

[11] M. Albrecht, H. Schily, C. Knauf, I. Schlangen, C. Schwalm, M. T. Rudrappa, M. Käske, “Space situational awareness using cooperative networks of phased-array radars”, NATO SET-297-RSM.

[12] D. Cerutti-Maori, J. Rosebrock, C. Carloni, M. Budoni, I. Maouloud, and J. Klare, “A Novel High-Precision Observation Mode for the Tracking and Imaging Radar TIRA – Principle and Performance Evaluation –“, Proc. 8th European Conference on Space Debris, Darmstadt, Germany, 2021.

[13] M. Budoni, C. Carloni, D. Cerutti-Maori, J. Rosebrock, I. Maouloud, and J. Siminski, “Investigation of different initial orbit determination methods for radar beam park experiments”, Proc. 8th European Conference on Space Debris, Darmstadt, Germany, 2021.

[14] M Budoni, C. Carloni, D Cerutti-Maori, and F. Piergentili, “Autonomous tracking mode with space observation radar: Initial Orbit Determination and Tracking”, ESA NEO and Debris Detection

Conference, 2019.

[15] [15] Herrick S., “Astrodynamics: orbit determination, space navigation, celestial mechanics (Vol. I)”. Van Nostrand Reinhold Co, 1971.

[16] Gibbs J., “On the determination of elliptic orbits from three complete observations Memoires National Academy of Science”, 4(2), 79–104, 1971.

[17] Kaiser H., Jehn R., “Determination of rough orbital elements from radar data in beam-park mode”, ESA-ESOC MAS working paper no. 377, 1996.

[18] https://astroscale.com/missions/elsa-d/

[19] Sarah Welch, Gregory Hogan, Delphine Cerutti-Maori, Simon Garrington, Robert Morrison, Matern Otten, Cees Bassa, Nick Pallecaros, Tonino Pisanu, Marco Martorella, “Long Baseline Bistatic Radar for Space Situational Awareness”, NATO SET-297-RSM.

[20] https://archive.lib.msu.edu/crcmath/math/math/c/c368.htm